





Article

Predicting *Cyperus esculentus* Biomass Using Tiller Number: A Comparative Analysis of Growth Models

Ya Ding ^{1,2,3,4} , Yan Lu ^{2,3,4}, Akash Tariq ^{2,3,4,5,6}, Fanjiang Zeng ^{1,2,3,4,*}, Yanju Gao ^{1,2,3,4}, Jordi Sardans ^{5,6} ,
Dhafer A. Al-Bakre ⁷  and Josep Peñuelas ^{5,6} 

- ¹ College of Ecology and Environment, Xinjiang University, Urumqi 830011, China; dingya@stu.xju.edu.cn (Y.D.); gaoyj@ms.xjb.ac.cn (Y.G.)
- ² Xinjiang Key Desert Plant Roots Ecology and Vegetation Restoration Laboratory, Xinjiang Institute of Ecology and Geography, Chinese Academy of Sciences, Urumqi 830011, China; luyan@ms.xjb.ac.cn (Y.L.); akash.malik786@mails.ucas.ac.cn (A.T.)
- ³ State Key Laboratory of Desert and Oasis Ecology, Xinjiang Institute of Ecology and Geography, Chinese Academy of Sciences, Urumqi 830011, China
- ⁴ Cele National Station of Observation and Research for Desert-Grassland Ecosystems, Hotan Prefecture 848300, China
- ⁵ Consejo Superior de Investigaciones Científicas, Global Ecology Unit, Centre de Recerca Ecològica i Aplicacions Forestals-Consejo Superior de Investigaciones Científicas-Universitat Autònoma de Barcelona (CREAF-CSIC-UAB), Bellaterra, 08193 Barcelona, Catalonia, Spain; j.sardans@creaf.uab.cat (J.S.); josep.penuelas@uab.cat (J.P.)
- ⁶ Centre de Recerca Ecològica i Aplicacions Forestals, 08193 Cerdanyola del Vallès, Catalonia, Spain
- ⁷ Department of Biology, College of Science, University of Tabuk, Tabuk 71421, Saudi Arabia; dalbakre@ut.edu.sa
- * Correspondence: zengfj@ms.xjb.ac.cn

Abstract: *Cyperus esculentus*, a drought-resistant Cyperaceae with ecological and economic value (stems/leaves as feed, tubers as oil source), stabilizes arid soils through its extensive root system. Understanding its biomass allocation strategies is crucial for comprehending carbon storage in arid environments. The results showed that allometric models best described leaf biomass, while Gompertz and logistic models provided superior accuracy (evaluated using R^2 , p -value, AIC, RMSE, and RSS) for estimating root, tuber, and whole plant biomass. In our study, the equilibrium biomass showed that underground (74.29 g and 64.22 g) was superior to aboveground (63.63 g and 58.72 g); and the growth rate showed the same result, underground (0.112 and 0.055) surpassed aboveground (0.083 and 0.046). The initial inflection point (POI1 = 11) suggests that leaves are prioritized in acquiring limited resources to support growth. In conclusion, the tiller number is a reliable predictor for developing robust biomass models for *C. esculentus*. The Gompertz model is best for leaves, roots, and total biomass, while the logistic model is optimal for predicting tuber biomass in arid areas. The tiller number is a reliable predictor for developing robust biomass models for *C. esculentus*. The research findings have supplied useful insights into the growth modifications, production potential, and management experience gained from *Cyperus esculentus* plant agriculture.

Keywords: *Cyperus esculentus*; biomass model; balanced biomass; growth rate; point of inflections



Academic Editor: Dengpan Xiao

Received: 14 March 2025

Revised: 19 April 2025

Accepted: 23 April 2025

Published: 27 April 2025

Citation: Ding, Y.; Lu, Y.; Tariq, A.; Zeng, F.; Gao, Y.; Sardans, J.; Al-Bakre, D.A.; Peñuelas, J. Predicting *Cyperus esculentus* Biomass Using Tiller Number: A Comparative Analysis of Growth Models. *Agriculture* **2025**, *15*, 946. <https://doi.org/10.3390/agriculture15090946>

Copyright: © 2025 by the authors.

Licensee MDPI, Basel, Switzerland.

This article is an open access article distributed under the terms and conditions of the Creative Commons Attribution (CC BY) license (<https://creativecommons.org/licenses/by/4.0/>).

1. Introduction

Cyperus esculentus, a member of the Cyperaceae family, has its aboveground parts utilized as forage for livestock, while the tubers serve as an important oil crop [1]. During the growth process, the biomass allocation of *C. esculentus* determines the growth potential

of various organs and the allocation facilitates the maintenance of growth under resource-limited conditions, as well as the adaptability and survival ability of crops [1–5]. In arid zones such as the Taklamakan Desert, water scarcity limits biomass partitioning, which directly affects carbon sequestration and agricultural productivity [6]. *C. esculentus* plays dual ecological (soil stabilization) and economic (forage and oil production) roles, yet region-specific biomass models remain underdeveloped. Therefore, in-depth research on biomass and allocation characteristics is crucial for comprehending plant performance, growth strategies, dynamic biomass monitoring, the development of comprehensive fertilizer strategies, and the refinement of agricultural techniques.

Biomass allocation is a crucial process in plant growth and development [7–10], determining how plants allocate limited resources to various organs based on the needs of different growth stages [11–13], for example, roots, stems, leaves, and other parts. During the growth and development of *Cyperus esculentus*, the biomass allocation pattern may be influenced by various environmental factors, especially the supply of water and nutrients, as well as changes in the growth environment [3–5,14]. Studies have shown that in resource-scarce environments, *Cyperus esculentus* typically exhibits a strategy of prioritizing the allocation of more biomass to the root system [15–17] to enhance the ability to absorb water and nutrients, which can improve survival and adaptability in scarce environments. The tiller number is a key indicator reflecting plant growth and biomass accumulation, directly related to plant growth dynamics and final yield [18,19]. Previous studies showed a close relationship between tiller number, biomass, and yield, which had a positive or negative effect on biomass accumulation and yield [19–21]. For *Cyperus esculentus*, the tiller ability plays an important role in the accumulation and distribution of biomass, and is one of the important parameters for its growth [1]. Therefore, to better understand the biomass allocation characteristics of *Cyperus esculentus*, it is necessary to establish an effective biomass model.

The biomass model can predict plant growth trends and biomass accumulation by quantifying the relationship between different growth parameters [22–24]. Many biomass models, such as linear models [25], allometric models [6,26,27], logistic models [28,29], Gompertz models [30] and so on, are widely used for estimating plant biomass in grasslands [31–33], economic crops [34,35], forests [22,36], and other areas. For example, According to Nie's [11] study, belowground biomass in *Shrub Biomes* in the northeastern Tibetan Plateau grows allometrically. Dou et al. (2019) used the allometric model to calculate aboveground biomass for *Caragana korshinskii* and *Sophora viciifolia*, which accurately predicted the link between biomass and growth parameters [36]. According to Gambín [37] and Pepler [38], grain (*Maize*, *Sorghum*, and *wheat*) biomass accumulation follows a logistic growth trend. Furthermore, Meade's [35] research discovered that the Gompertz model may characterize *maize seed* biomass accumulation. Furthermore, tiller quantity is an important metric for plant growth, and the composition and dynamics of tiller populations are the basis for population quality and high and steady crop yields [20,39,40]. Some scholars have found a close correlation between the tiller number and leaf biomass in *Stipa breviflora* [41]. Kren. J's [42] research reveals a significant correlation between the tiller number, grain yield, and dry weight per unit area of aboveground biomass ($R > 0.81^*$). Arvid Boe's research further confirms the previous conclusion that the tiller number always has a positive direct impact on biomass and yield [43]. For *Cyperus esculentus*, research has verified that their growth characteristics conform to logistic characteristics [29]. However, the quantitative relationship between growth parameters and biomass accumulation has not been fully considered, and the applicability of the model also needs further verification due to regional differences.

In summary, considering the tillering characteristics and growth mode of *Cyperus esculentus*, three existing biomass models (including the allometric model, logistic model, and Gompertz model) are used for prediction. We establish strong hypotheses: (1) the number of tillers is a key factor in predicting the biomass of *Cyperus esculentus*; (2) due to the unique growth characteristics and resource allocation patterns of cattails, constructing a Gompertz model using tiller number can effectively predict the biomass of *C. esculentus*. Thus, the tiller number was used to build a biomass model, and different biomass models were compared and analyzed. This not only optimized the plant biomass prediction method, but also revealed the underground priority resource allocation strategy for cattail, which provides a scientific basis for ecological restoration, carbon sink management, and plant ecological adaptation strategies in arid regions.

2. Materials and Methods

2.1. Experimental Area and Sample Collection

This study was conducted on the northern margin of the Taklamakan Desert (41°36' N, 86°3' E), in a transition zone between a desert and oasis. This area features a temperate continental arid climate characterized by scant rainfall and ample sunlight. The region receives an average of 3045 h of annual sunshine, with a frost-free period averaging 180 days. The groundwater level is more than 14 m below the ground. With an average annual air temperature of 18 °C, the area receives only 57 mm of rainfall annually, contrasted by a maximum annual evaporation rate of 2788.2 mm, indicating that precipitation is far less than evaporation. The predominant soil type in this region is sandy, and the experimental zone, located at the forefront of the desert, hosts sparse vegetation. The physical and chemical properties of the 0–30 cm soil are as follows: field water holding capacity: 18%, bulk density of soil: 1.58 g/cm³, content of organic matter: 1.58 g/cm³: 4588.55 mg/kg, hydrolysed nitrogen content: 28.41 mg/kg, available phosphorus content: 9.89 mg/kg, available potassium content: 73.783 mg/kg, and pH: 7.6.

This study was conducted from June to October 2020 and 2021, at three independent large sample plots, each with the size of 15 m × 15 m; within each large sample plot, five 1 m × 1 m plots were systematically divided along the diagonal direction, and the diagonal division method ensured the spatial distribution uniformity of the samples while avoiding the interference of edge effects on the data. Five complete plants were selected as samples from each small plot using a simple random sampling method; a total of 75 plants were collected for each sampling (3 large sample plots × 5 small sample plots × 5 plants), with a sampling period set to once every 30 days, for a total of 4 samplings, sampling design is shown in Figure 1. During the sampling, the tiller number of the selected plants was recorded, and the entire plant was excavated from the sampling site to obtain test plants. The root systems were dug up as deeply as possible to ensure their completeness. These samples were then transported to the laboratory for cleaning and drying. They were subsequently kept at a constant temperature of 80 °C for 24 h until they reached a constant weight.

The procedure for counting tillers involved direct observation, focusing on the number of tillers on plants, excluding the main stem. The dry weight of the plants was determined for the following components: leaf biomass (LBM), root biomass (RBM), and tuber biomass (TuBM). The total biomass of leaves, roots, and tubers was then used to calculate the total plant biomass (ToBM).

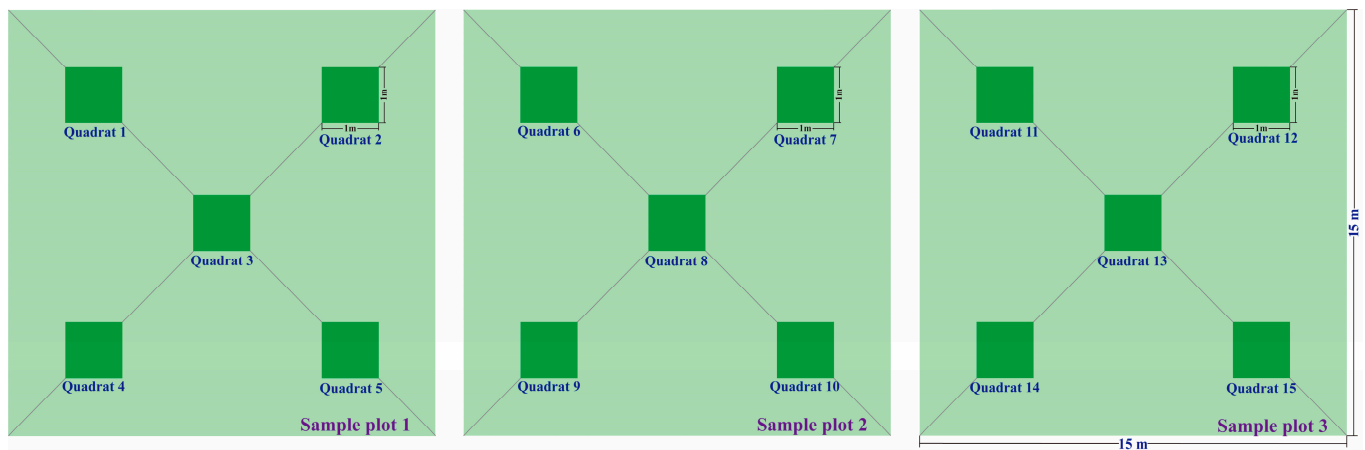


Figure 1. Distribution map of sample collection in the research area.

2.2. Establishment and Goodness of Fit Evaluation

This study used the “caret” package from R 4.2.1 (R Core Team, 2022) [44] to conduct a simple cross-validation and the 7:3 ratio was used to classify the data [45]. Approximately 70% of the data (2/3 of the data) was used to build a model, including 420 leaves, roots, tubers, and total biomass data. The remaining 30% (1/3 of the data) was used to validate the model, which includes 180 leaves, roots, tubers, and total biomass data. Finally, the tiller number was used as the independent variable, with leaf, root, tuber, and whole plant biomass as dependent variables to construct allometric models [46] (1), logistic models [47] (2), and Gompertz models [48] (3), to estimate the leaf, root, tuber, and whole plant biomass of *C. esculentus*.

$$BM = a \times TN^b \quad (1)$$

$$BM = k / (1 + \exp(a - b \times TN)) \quad (2)$$

$$BM = k \times \exp(-\exp(a - b \times TN)) \quad (3)$$

Note: *TN* represents the number of tillers; *BM* refers to leaves, roots, tubers, and total biomass; *a*, *b*, and *k* are constants.

This study is based on indicators related to goodness of fit and aims to elucidate discrepancies in goodness of fit between the allometric model (1), logistic model (2), and Gompertz model (3), to assess the relative merits and shortcomings of each model. The goodness of fit indexes are primarily defined by the adjusted coefficient of determination (R^2 and R^{2*} , Formulas (4) and (5)), level of significance (*P*), root mean square error (RMSE, Formula (6)), Akaike information criterion (AIC, Formula (7)), and residual (RSS, Formula (8)). Based on previous research [36,49–52], the model with the highest R^{2*} and lowest RMSE, AIC, and RSS was selected as the optimal biomass estimation model. Additionally, the effectiveness of the most efficient estimation model for assessing plant biomass in arid regions was validated through the construction of a linear regression equation, correlating estimated and measured values.

$$R^2 = 1 - \frac{\sum_{i=1}^n (y_i - \hat{y}_i)^2}{\sum_{i=1}^n (y_i - \bar{y}_i)^2} \quad (4)$$

$$R^{2*} = 1 - \frac{n-1}{n-q} (1 - R^2) \quad (5)$$

$$RMSE = \sqrt{\frac{\sum (y_i - \bar{y}_i)^2}{(n - 1)}} \quad (6)$$

$$AIC = -2\ln(-n/2\ln(RS/n)) + 2q \quad (7)$$

$$RSS = \sum_{i=1}^n (y_i - \hat{y}_i)^2 \quad (8)$$

Note: y_i , \bar{y}_i , and \hat{y}_i represent measured, estimated, and average biomass values, respectively, RSS represents the sum of squared residuals, and n and q indicate the number of samples and model variables, respectively.

2.3. The Significance of Model Parameters

The allometric model follows a power-law distribution [53]. The “a” is a constant and “b” is the allometric growth index, where $b = 1$ indicates isokinetic growth and $b \neq 1$ indicates allometric growth [54]. In addition, the parameter “b” can partially reflect the trade-off relationship between plant biomass formation and tiller numbers.

The logistic and Gompertz models are frequently employed to demonstrate biological growth in populations that dwell in environments with limited resources. In these models, the value of “a” is a constant parameter, and the values of “k” and “b” have been discovered to have considerable effects on ecological processes [55,56]. The variable “k”, which represents the equilibrium biomass, shows a progressive increase from the initial growth phase to the accelerated growth phase as a function of the tiller number (tiller number inflection point POI₁); with the limitation of available resources, as the environment approaches or reaches its maximum capacity, biomass gradually approaches equilibrium (tiller number inflection point POI₂). The variable ‘b’ reflects the equilibrium growth rate, which is highly connected with plant development and represents the growth rate of biomass in an optimum environment [49].

2.4. Statistical Analysis

This study utilized SPSS version 26.0 to analyze biomass data and describe variations in the tiller number, leaf biomass, root biomass, tuber biomass, and total plant biomass. Additionally, we assessed the correlation between the tiller number and the biomass of different organs. Using the tiller number as the independent variable and the biomass of different organs as dependent variables, we constructed the allometric, Gompertz, and logistic models. Among these models, the “caret” package in R 4.2.1 (R Core Team, 2022) was employed to ensure that the modeling and validation datasets remained relatively independent. Graphical visualization analysis in Origin 2021 was utilized to identify the tiller number inflection point values (POI) corresponding to different stages of biomass growth, as described by the Gompertz and logistic models. Furthermore, this study calculated R^{2*} , R^2 , p values, RMSE, and AIC using R version 4.1.1 to comprehensively evaluate the goodness of fit of the models, and employed linear regression between predicted biomass values and measured values to determine the predictive effectiveness of the models.

3. Results

3.1. Basic Description and Biomass Allocation

In our study (Table 1), the minimum number of tillers recorded was 1, the maximum was 144, and the mean number of tillers was 25.00 ± 0.89 throughout the reproductive period. This variability may reflect the adaptive strategies of plants under different environmental conditions. The average values of leaf biomass, root biomass, tuber biomass, and total biomass were 18.41 ± 0.82 g, 7.42 ± 0.36 g, 14.18 ± 0.88 g, and 40.00 ± 1.88 g,

respectively. The allocations of leaf, root, and tuber biomass represented 46.03%, 18.55%, and 35.45% of the total biomass, respectively. This result may be due to the fact that leaves are key for photosynthesis, and higher leaf biomass allocation may enhance light capture during reproduction, supporting tuber growth; as storage organs, tubers are vital for reproduction and survival; the lower root biomass suggests that plants prioritize aboveground growth during reproduction. During the growth and development period, the biomass of leaves, roots, tubers, and the entire plant exhibited a trend of initially increasing and then decreasing (Figure 2). Notably, August represented a critical period for the accumulation of biomass in leaves, roots, and tubers, and it should be ensured that plants receive sufficient light, water, and nutrients to maximize biomass accumulation.

Table 1. The growth parameter characteristics of *Cyperus esculentus*.

Index	Min Value	Max Value	Mean Value	Standard Error	Allocation Proportion
Tiller numbers	1.00	144.00	24.91	0.89	-
Leaf biomass	0.31	97.86	18.41	0.82	46.03%
Root biomass	0.21	65.87	7.42	0.36	18.55%
Tuber biomass	0.00	96.08	14.18	0.88	35.45%
Total biomass	0.55	217.39	40.00	1.88	-

Note: Tiller numbers (TN), leaf biomass (LBM), root biomass (RBM), tuber biomass (TuBM), total biomass (TOBM).

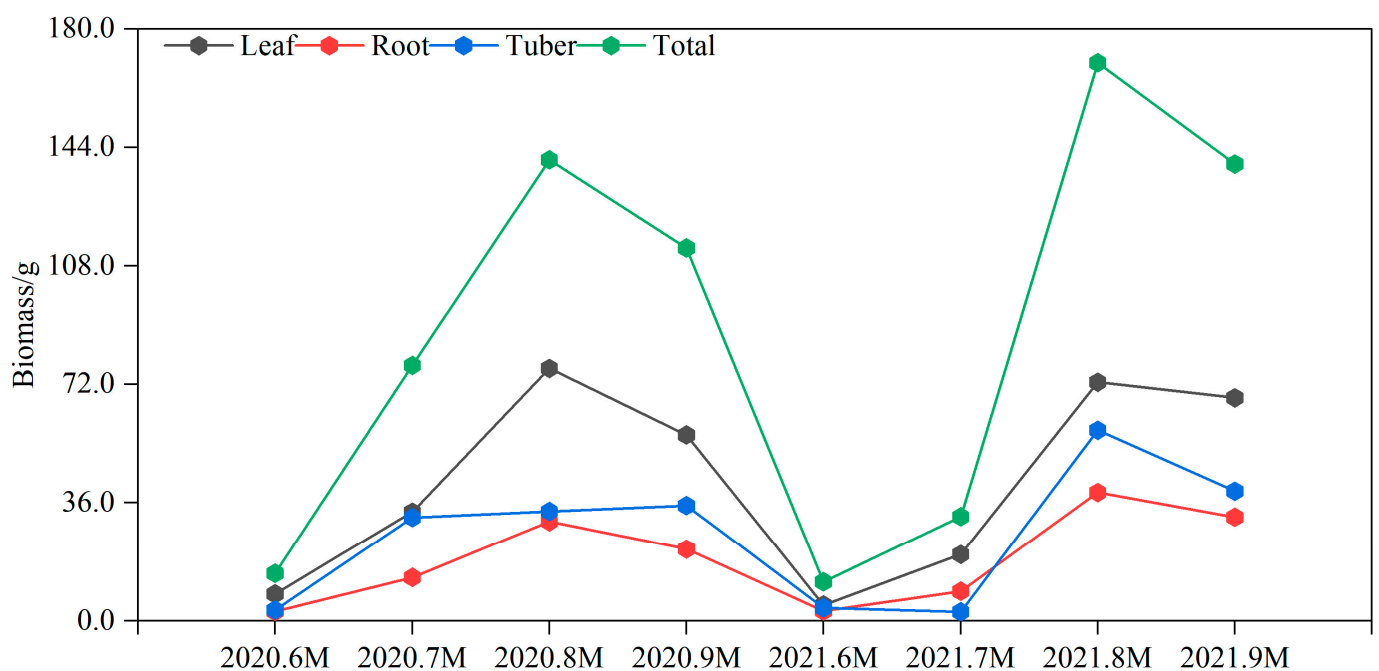


Figure 2. Dynamic characteristics of leaf, root, tuber, and total biomass of *Cyperus esculentus* from 2020–2021.

The analysis of the correlation results (Table 2) revealed that the number of tillers and the biomass of different organs were closely related (correlation coefficient > 0.50). The number of tillers exhibited a strong correlation with leaf biomass ($p < 0.001$), with a coefficient of 0.853; this may be due to the fact that an increase in the number of tillers is usually accompanied by an increase in the number of leaves, thus increasing the effective area of photosynthesis. The number of tillers also showed significant relationships with root (0.721), tuber (0.567), and total biomass (0.773) ($p < 0.01$), which may reflect the balancing strategies of plants in resource allocation. The number of tillers was more closely related

(correlation coefficient > 0.720) to leaf, root, and total biomass than to tuber biomass. In conclusion, the strong correlation between the tiller number and leaves, roots, and total biomass indicates that the tiller number is an important driving factor for plant growth and resource allocation. Biomass models based on the tiller number are of great scientific and practical significance and can provide important support for agricultural management.

Table 2. The correlation between basic parameters and biomass.

Index	Tiller Numbers	Leaf Biomass	Root Biomass	Tuber Biomass	Total Biomass
Tiller numbers	1.00				
Leaf biomass	0.853 ***	1.00			
Root biomass	0.721 **	0.831 ***	1.00		
Tuber biomass	0.567 **	0.749 **	0.663 **	1.00	
Total biomass	0.773 **	0.924 ***	0.824 ***	0.915 ***	1.00

Note: ***: $p < 0.001$, highly significant; **: $p < 0.01$, extremely significant.

The biomass of different organs and total biomass were linearly correlated ($R^2 = 0.924$, $p < 0.001$; $R^2 = 0.821$, $p < 0.001$; $R^2 = 0.915$, $p < 0.001$) (Figure 3A–D). This strong correlation supports the interdependence between leaf, root, tuber, and total biomass. The confidence intervals for the biomass of leaves, roots, and tubers were 92.4%, 82.1%, and 91.5%, with average values of 18.41 g, 7.42 g, and 14.18 g, respectively. Therefore, a significant portion of the biomass of *Cyperus esculentus* was concentrated in the leaves. Additionally, there was a significant linear correlation between aboveground and underground biomass, indicating that underground biomass increased as aboveground biomass increased ($R^2 = 0.811$, $p < 0.001$) (Figure 3D).

3.2. Construction of Different Biomass Models

According to Table 3, the biomass model constructed using the tiller number as the independent variable and biomass as the dependent variable demonstrates a good goodness of fit, with $R^2 > 0.65$. These results further validate the feasibility of constructing biomass models based on tiller numbers. Furthermore, when comparing the allometric model, the logistic model ($0.740 < R^2 < 0.878$) and the Gompertz model ($0.738 < R^2 < 0.886$) exhibited a better goodness of fit, with relatively small differences between the two. Although both models achieved high significance levels ($p < 0.001$) in estimating biomass for herbaceous plants in arid areas, the Gompertz model showed the highest results.

Table 3. Comparison of goodness of fit between different models for estimated biomass.

Index	Models	Parameters			Goodness-of-Fit Test						
		a	b	k	R^2	R^{2*}	p	Q	RMSE	AIC	RSS
LBM	$LBM = a \times (TN)^b$	1.388	0.844	-	0.837	0.836	<0.0001	2	9.617	801.926	15,151.86
	$LBM = k / (1 + \exp(a - b \times TN))$	2.825	0.083	59.616	0.878	0.877	<0.0001	3	9.43	799.716	14,967.01
	$LBM = k \times \exp(-\exp(a - b \times TN))$	1.304	0.046	64.856	0.886	0.885	<0.0001	3	9.312	788.744	14,081.93
RBM	$RBM = a \times (TN)^b$	0.532	0.826	-	0.78	0.779	<0.0001	2	5.994	645.918	6368.82
	$RBM = k / (1 + \exp(a - b \times TN))$	2.662	0.086	18.946	0.828	0.826	<0.0001	3	5.904	638.997	6128.59
	$RBM = k \times \exp(-\exp(a - b \times TN))$	1.227	0.049	20.465	0.83	0.828	<0.0001	3	5.861	636.54	6045.50

Table 3. Cont.

Index	Models	Parameters			Goodness-of-Fit Test						
		a	b	k	R ²	R ² *	p	Q	RMSE	AIC	RSS
TuBM	TuBM = $a \times (TN)^b$	0.296	1.281	-	0.658	0.655	<0.0001	2	18.689	1049.292	59,882.31
	TuBM = $k/(1 + \exp(a - b \times TN))$	3.993	0.112	65.082	0.740	0.739	<0.0001	3	15.384	967.379	37,989.40
	TuBM = $k \times \exp(-\exp(a - b \times TN))$	1.795	0.055	76.296	0.738	0.737	<0.0001	3	15.703	977.13	40,104.14
ToBM	TOBM = $a \times (TN)^b$	2.934	0.846	-	0.738	0.737	<0.0001	2	24.665	1157.94	109,506.20
	TOBM = $k/(1 + \exp(a - b \times TN))$	3.027	0.101	112.865	0.805	0.803	<0.0001	3	23.764	1146.535	101,646.89
	TOBM = $k \times \exp(-\exp(a - b \times TN))$	1.424	0.057	121.581	0.809	0.807	<0.0001	3	23.293	1137.33	97,658.60

Note: LBM: leaf biomass; RBM: root biomass; TuBM: tuber biomass; ToBM: total biomass. TN indicates tiller numbers. a, b, and k are constants. R² and R²* indicates coefficient of determination and adjusted coefficient of determination. p-value indicates the significance of the model, $p < 0.001$, highly significant; RMSE indicates root mean square error. AIC indicates akaike information criterion. RSS: residual sum of squares.

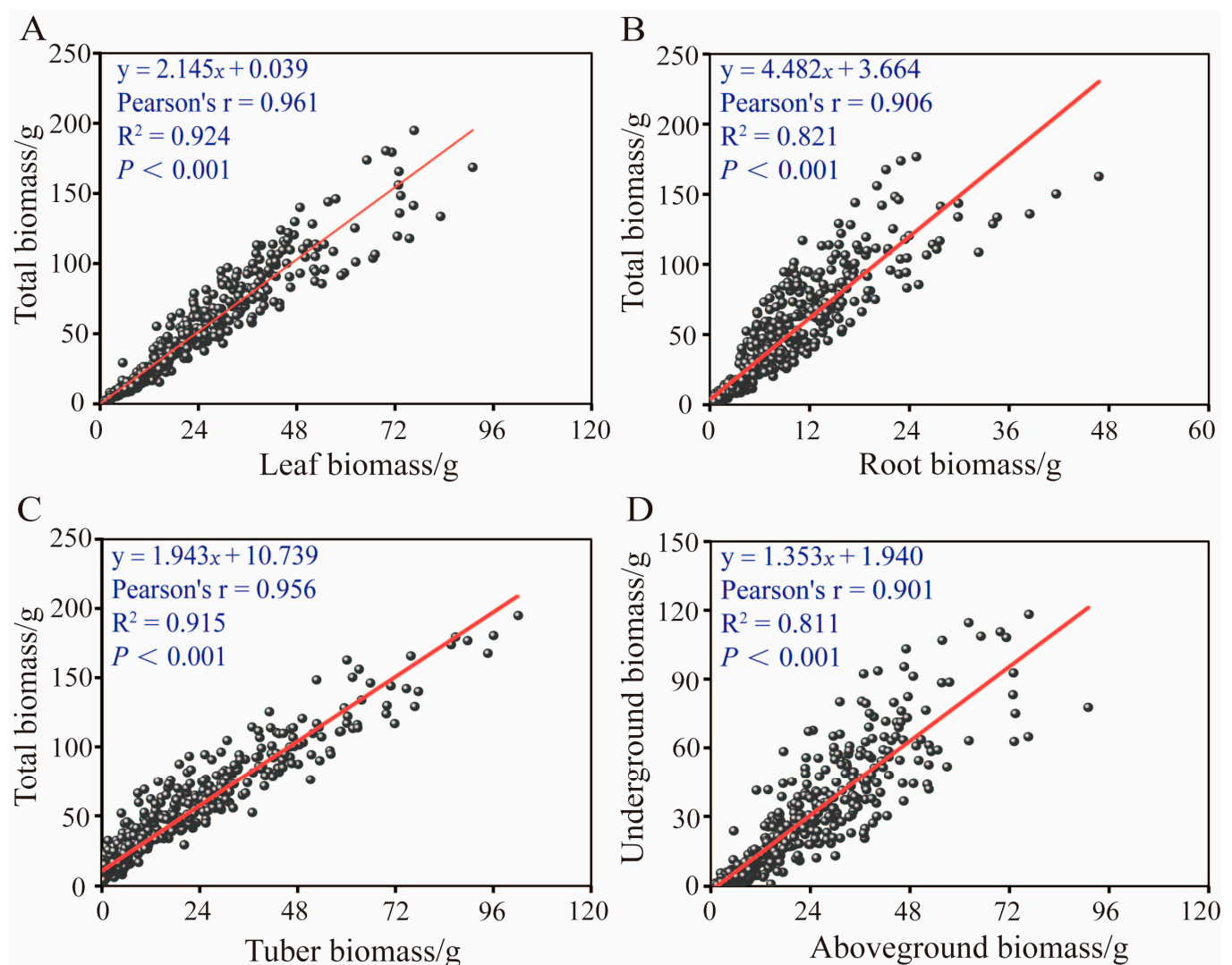


Figure 3. The correlation between aboveground and underground biomass. (A) represents the leaf mass ratio: leaf biomass/total biomass; (B) represents the root mass ratio: root biomass/total biomass; (C) represents the tuber mass ratio: tuber biomass/total biomass; (D) represents root/shoot ratio.

R^2 values were obtained for estimating leaf (0.886), root (0.830), and total biomass (0.809), along with lower RMSE values (9.312, 5.861, and 23.293, respectively) and lower AIC values (788.744, 636.540, and 1137.330, respectively). However, the logistic model demonstrated higher accuracy for tuber biomass estimation, with an R^2 of 0.740, lower RMSE (15.384), and lower AIC (967.379). In summary, the different characteristics of plant growth and development are superior, and the fitting effect of biomass for different organs also varies. Among them, Gompertz models for leaf, tuber, and whole plant biomass have the best performance due to their high R^2 (0.89, 0.83, 0.81), low RMSE (9.31, 5.86, 23.29), low AIC (788.744, 636.54, 1137.33), and low RSS (1481.93, 6045.50, 97,658.60). The logistic model for tuber biomass has the best estimation performance due to a high R^2 (0.740) and low RMSE (15.38), AIC (967.38), and RSS (37989.40); this result reflects the heterogeneity of different organ growth strategies. In general, logistic and Gompertz models are superior to the allometric growth model for biomass estimation in ecological contexts, and more suitable for estimating the biomass of *Cyperus esculentus* in this region.

3.3. Comparison and Validation of Measured and Estimated Values of Different Biomass Models

As shown in Figure 4, the regression lines of the estimated and measured values of these three models closely align with the 1:1 reference line. The slope and intercept of the linear regression equations are also relatively similar, indicating the models possess good predictive power. The slopes of the linear regressions when estimating leaf, root, tuber, and total biomass are as follows: Gompertz model (LBM = 0.852, RBM = 0.741, TuBM = 0.829, ToBM = 0.747) > logistic model (LBM = 0.830, RBM = 0.729, TuBM = 0.804, ToBM = 0.729) > allometric model (LBM = 0.779, RBM = 0.652, TuBM = 0.721, ToBM = 0.660). For the intercepts of the linear regressions, the values are as follows: Gompertz model (LBM = 3.549, RBM = 1.611, TuBM = 2.913, ToBM = 7.710) < logistic model (LBM = 4.352, RBM = 1.814, TuBM = 3.663, ToBM = 9.298) < allometric model (LBM = 4.866, RBM = 2.195, TuBM = 4.998, ToBM = 12.241). In summary, the predicted and measured values of biomass based on the logistic and Gompertz models demonstrate more concentrated scatter points, higher agreement, and a more uniform distribution around the reference line (1:1) compared to the allometric model.

3.4. Comparison of the Ecological Significance of Different Biomass Models

Figure 5 illustrates that the allometric growth model predicts a 'J'-shaped biomass growth trend with increasing tillers; the allometric growth model can only describe power-law relationships and cannot capture the S-shaped biomass growth trend (such as asymptotic equilibrium under constrained resources). Leaf biomass demonstrates the greatest goodness of fit ($R^2 = 0.837$) compared to root biomass ($R^2 = 0.780$), tuber biomass ($R^2 = 0.658$), and whole plant biomass ($R^2 = 0.738$). Compared to allometric growth, Gompertz and logistic models quantify the dynamic biomass growth process through parameters 'k' (equilibrium biomass) and 'b' (equilibrium growth rate). In our study, the logistic and Gompertz models indicate that biomass production increases in an S-shaped pattern as the number of tillers rise. In the logistic model, the balanced biomass of tubers ($k = 65.082$ g) was greater than that of leaves ($k = 59.616$ g) and roots ($k = 18.946$ g). The balanced growth rates for these organs can be described as follows: tuber ($b = 0.112$) > root ($b = 0.086$) > leaf ($b = 0.083$). Consistent results were observed in the Gompertz model, where balanced biomass was expressed as tuber ($k = 79.296$ g) > leaf ($k = 67.221$ g) > root ($k = 20.436$ g), with growth rates indicated as tuber ($b = 0.055$) > root ($b = 0.049$) > leaf ($b = 0.046$).

The points of inflection (POI) in the models indicate specific moments in the growth process of the plants, where the rate of biomass growth begins to slow down or acceler-

ate [57–59]. The allometric growth model cannot identify the point of inflection (POI) of biomass growth, whereas the Gompertz and logistic models reveal the priorities of resource allocation of the different organs through POI_1 and POI_2 . In our study, leaf biomass experienced significant increases at a tiller count of 12 (POI_1) and stabilized at a count of 84 (POI_2). Similarly, root and tuber biomass exhibited notable increases at tiller counts of 12 and 15 (POI_1) and reached equilibrium at counts of 73 and 76 (POI_2). Overall, when comparing the growth patterns of different organs, aboveground biomass growth was characterized more by the allometric growth pattern than belowground biomass. In the logistic model, the equilibrium biomass of different organs was expressed as tubers (65.082 g) > leaves (59.616 g) > roots (18.946 g), with the growth rate expressed as tubers (0.112) > roots (0.086) > leaves (0.083). In the Gompertz model, the highest equilibrium biomass was found in tubers (79.296 g), followed by leaves (67.221 g) and roots (20.436 g); the growth rates were tuber (0.055) > root (0.049) > leaf (0.044). This indicates that, in this region, the growth of tubers with higher biomass is often prioritized over that of leaves and roots to achieve maturity.

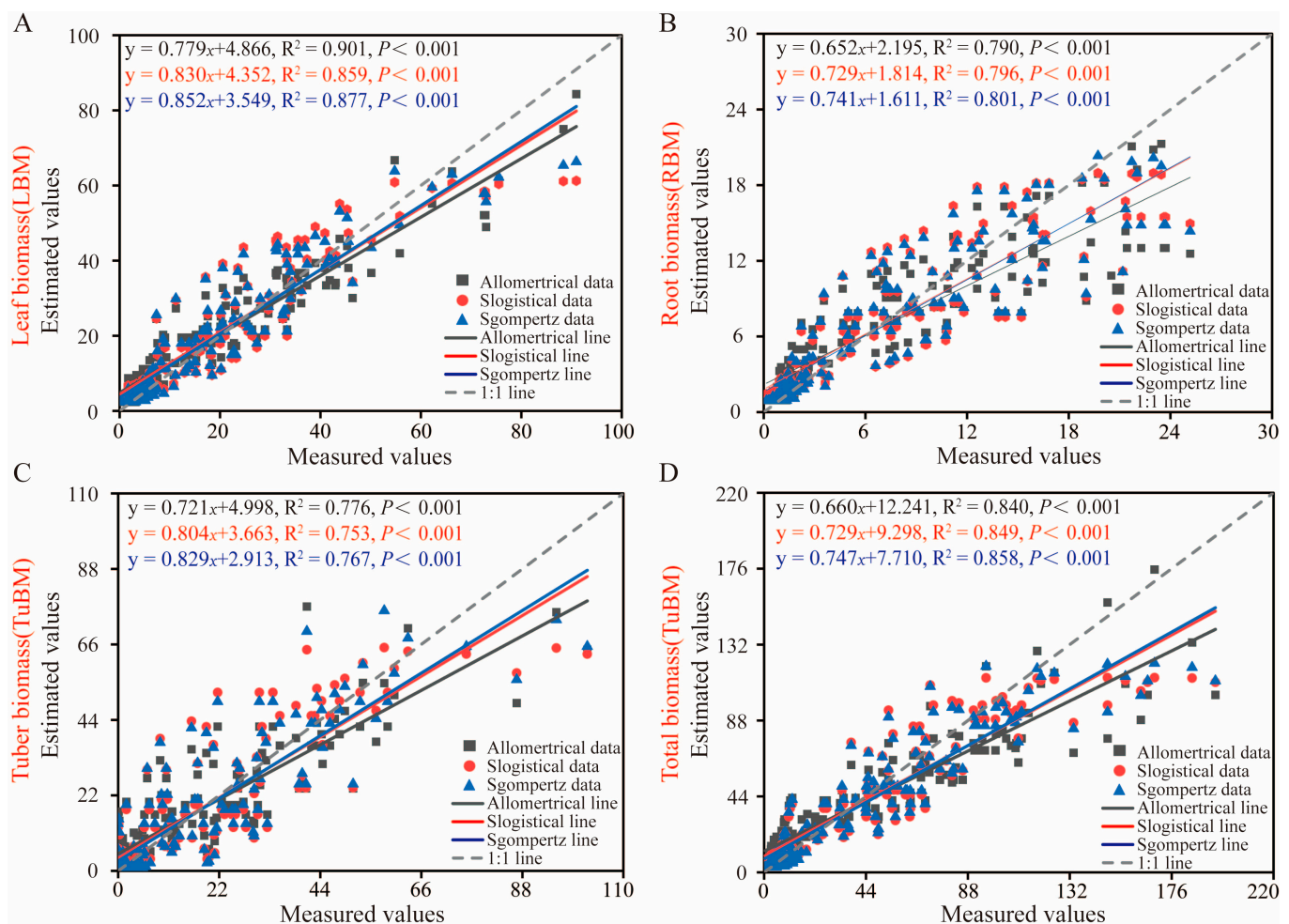


Figure 4. The relationship between measured and estimated values of different models. (A) represents the linear relationship between measured and estimated values of leaf biomass; (B) represents the linear relationship between measured and estimated values of root biomass; (C) represents the linear relationship between measured and estimated values of tuber biomass; (D) represents the linear relationship between measured and estimated values of total biomass.

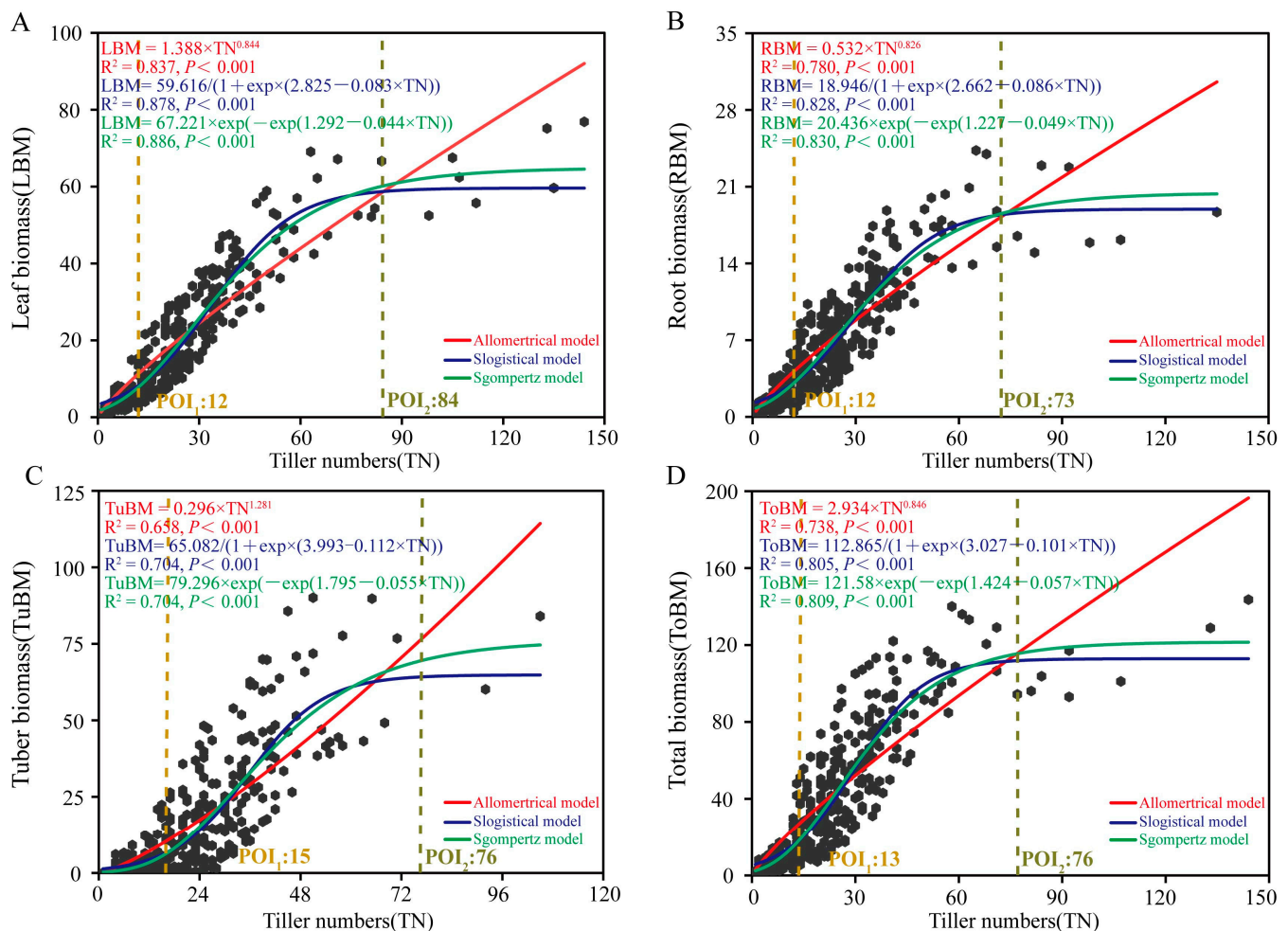


Figure 5. Comparison of biomass estimation models for different organs. (A) indicates the growth model of tiller number and leaf biomass; (B) indicates the growth model of tiller number and root biomass; (C) indicates the growth model of tiller number and tuber biomass; (D) indicates the growth model of tiller number and total biomass.

4. Discussion

4.1. Introduction of Parameters to Explain Biomass Models

This allometric growth model has been extensively validated in previous studies [60,61]. However, owing to variations in regional characteristics, environmental factors, and plant properties, allometric models exhibit relatively poor stability [62,63]. This variability underscores the need for region-specific models for agricultural practices and ecological assessments. The logistic and Gompertz models, which quantify equilibrium biomass and growth rates through parameters “k” and “b” [48,59], offer different insights into plant growth dynamics. According to our analysis, the balanced biomass of leaves, roots, and tubers in the logistic model (59.61 g, 18.946, and 65.082 g, respectively) was lower than that in the Gompertz model (64.856, 20.465, and 76.296 g, respectively). This result is consistent with Carini’s research [64], which suggests that the Gompertz model outperforms the logistic model in estimating balanced biomass (k) for different organ biomass. When calculating the equilibrium biomass, under both models, the highest proportion of *Cyperus esculentus* biomass was allocated to tubers (57.66% and 62.75%), which reflects adaptability to arid environments, survival strategies for optimizing resource allocation, and economic value. This contrasts with Ma’s [59] research, which found that the equilibrium biomass of *C. korshinskii* and *S. psammophila* leaves (25.43 g and 169.37 g, respectively) was less than

that of stems (245.16 g and 1169.24 g, respectively). This may indicate that drought-tolerant shrubs invest more biomass in their stems.

Balanced growth rates are key indicators of a plant's growth strategy and response to environmental pressures. Plants optimize resource allocation by varying organ growth rates, which are crucial for adaptation and reproduction when resources are limited [65–67]. Studies by Ma [59] and Bem [58] discovered that the balanced growth rate of leaves is typically higher than that of stems, suggesting that leaf maturation may be prioritized in terms of growth rate, underscoring the importance of leaves during the early phases of plant growth [68]. Additionally, research has shown that, under drought conditions, plants may invest more in their root systems to extract water and nutrients from the soil, thereby favoring underground biomass growth [69,70]. In our study, the balanced growth rates of different organs of *Cyperus esculentus* in arid areas were found to be lower in leaves (0.083, 0.044) than in tubers (0.112, 0.055) and roots (0.086, 0.049). These results indicate that the tubers of *Cyperus esculentus* are grown more easily than the leaves, mainly because tubers are the main mode of reproduction, revealing the adaptability of cattails to arid environments, demonstrating that their survival strategies adapt to optimize resource allocation, and highlighting the key role of asexual reproduction in this process [1].

4.2. Response of Inflection Points to Biomass Change Trends

The logistic and Gompertz growth curves reflect the growth trend of plants, and points of inflection explain the possible changes in the resource allocation strategies of plants at different growth stages, which is crucial for understanding plant responses to environmental changes and resource availability [30,59,71]. In our study, the leaf biomass POI_1 occurred at a tiller number of 11, which was smaller than the POI_1 for the root (12) and tuber (16) biomass. This discrepancy may be related to the theory of optimal biomass allocation [72], further confirming previous research conclusions that leaf biomass enters the rapid growth stage earlier than other organs [8].

Compared to the allometric model, the logistic and Gompertz models depict a transition from mild to rapid biomass increase at confirmed POI_1 , while POI_2 represents the approaching asymptotic value of biomass [30,58]. These findings indicate intraspecific competition and resource limitations. Our study revealed a significant increase in leaf biomass when the number of tillers exceeded 11 (POI_1), which marked a critical turning point in plant development. When the number of tillers reached 84 (POI_2) and 112 (POI_3), the leaf biomass approached an asymptotic value (Figure 5A). This phenomenon has been validated by previous studies, which indicate that to support their rapidly expanding canopy and enhance photosynthetic efficiency, plants prioritize resource allocation to leaf growth during the early growth stages [73]. Root biomass exhibited significant growth, beginning at tiller 14 (POI_1) and stabilizing at POI_2 values of 73 and 108 (Figure 5B). Tuber biomass also increased from POI_1 , with near asymptotic values at POI_2 (TN = 76) and POI_3 (TN = 101) (Figure 5C). Overall, these results suggest that, as plants mature, their resource allocation strategies shift increasingly toward underground parts, such as tubers and roots [74]. This redistribution of resources is crucial for the survival of plants in extreme environmental conditions, such as drought [49,75]. Overall, the logistic and Gompertz models measure the change from POI_1 (accelerated growth value) to POI_2 (asymptotic value), which not only reveals the growth dynamics and resource allocation strategies of *C. esculentus* but also reflects the adaptability of plants to environmental changes. In addition, identifying key growth periods through inflection points and optimizing planting and management strategies can improve the yield of *C. esculentus*.

4.3. Comparison of Differences Between Different Models

The allometric, Gompertz, and logistic models provide a quantitative description of crop growth dynamics by quantifying the growth rates of various parts of the plant body, which helps to better understand the growth and development laws, adaptation strategies, and ecological characteristics of plants [49]. Deprá studied the relevance of logistic models for the growth of *Creole maize* cultivars [71]; Bem's research examined how Gompertz and logistic models suit the physical properties of sunflowers [23]; some scholars used logistic and Gompertz models to simulate and analyze the growth of young *Caryophyllum* seedlings, and found that the logistic model outperformed the Gompertz model [70]. Similar to previous results, Gompertz and logistic models surpassed allometric growth models in estimating *C. esculentus* biomass.

Various biomass estimating models show varied characteristics, owing to variances in their goodness of fit and prediction abilities, which have a substantial influence on agricultural operations (optimizing irrigation and fertilization) and species ecology [76,77]. In our study, the Gompertz model (R^2 : 0.886, 0.830, 0.809) performed better than the logistic model (R^2 : 0.878, 0.828, 0.805) in terms of leaf, root, and total biomass. Compared with the Gompertz model ($R^2 = 0.738$), the logistic model ($R^2 = 0.740$) performs the best in estimating tuber biomass. These results indicate that the Gompertz model is more suitable for management decisions of forage in agricultural production, whereas the logistic model may be more suitable for the agricultural management of tubers, but field data were limited to two growing seasons; long-term validation under variable rainfall regimes is needed to assess model robustness. In addition, by identifying the inflection points (POI₁, POI₂, POI₃) of the Gompertz and logistic models, the key growth stages of *Cyperus esculentus* were determined, which has practical value for large-scale planting and management (fertilization and irrigation).

The distinctions in the models indicate the allocation characteristics of aboveground biomass [51,78]. Previous research has mostly shown the allocation characteristics of various organs (leaves, stems, and roots) and aboveground and belowground biomass by analyzing the association between aboveground allometry and R/S [9,33,79]. In our study, the R/S and tuber allometric growth indices were both >1 , indicating that the growth of tubers was better than that aboveground, and more biomass tended to be allocated underground. Except for the allometric, logistic, and Gompertz models, their biomass allocation characteristics and adjustment to the environment were emphasized by balancing the biomass and growth rate parameters [28,51]. In our study, the equilibrium biomass and equilibrium growth rate parameters in the model showed different changes due to the model, and the equilibrium biomass of different organs was manifested as tubers (79.296 and 65.82) $>$ leaf (67.221 and 59.616) $>$ root (20.436 and 18.946), indicating that *C. esculentus* distributes more biomass underground, potentially obtaining more water and nutrients, while also reflecting its adaptability to arid environments. In addition, the balanced growth rate of *C. esculentus* in different organs was manifested as tuber (0.055 and 0.112) $>$ root (0.049 and 0.086) $>$ leaf (0.044 and 0.083), and the difference in the balanced growth rate reveals the growth pattern of *Cyperus esculentus*, that is, the leaf biomass increases rapidly in the early stages of *C. esculentus* growth, while in the mature stage, more biomass is allocated underground.

5. Conclusions

Our comparative analysis of biomass modeling approaches for *Cyperus esculentus* reveals key findings: firstly, prioritizing the estimation of aboveground biomass using the tiller number as a key predictor significantly improved model reliability. Secondly, the logistic and Gompertz models showed exceptional competitiveness in terms of goodness-of-

fit metrics, but the biomass model differed due to differences in plant organs: the Gompertz model exhibited superior prediction accuracy for leaf biomass, root biomass, and total plant biomass; conversely, the logistic model outperformed other models in tuber biomass estimation, reflecting its strength in modeling saturation dynamics typical of belowground storage organs. Thirdly, the proportion of balanced biomass of underground biomass (tubers and roots) (74.29 g and 64.22 g) was significantly higher than aboveground biomass (63.63 g and 58.72 g), suggesting an ecological adaptation strategy of prioritizing resource allocation to underground organs in arid environments for *Cyperus esculentus*. Finally, POI₁ (TN = 11) guides leaf growth and agronomic management, while POI₂ (TN = 84) benefits tuber propagation and agronomic management.

Author Contributions: Y.D.: conceptualization, investigation, formal analysis, and writing—original draft. Y.L.: conceptualization and supervision. A.T.: conceptualization, writing—review and editing, supervision, and project administration. F.Z.: conceptualization, writing—review and editing, supervision, and project administration. Y.G.: conceptualization and supervision; J.S.: conceptualization and supervision; D.A.A.-B.: conceptualization and supervision; J.P.: conceptualization and supervision. All authors have read and agreed to the published version of the manuscript.

Funding: The research in this paper was financially supported by the Key Research and Development of Xinjiang Uygur Autonomous Region (2022B02040), and the APC was funded by the Key Research and Development of Xinjiang Uygur Autonomous Region.

Data Availability Statement: The original contributions presented in this study are included in the article. The data presented in this study are available on request from the corresponding author. The data are not publicly available due to privacy issues.

Conflicts of Interest: No conflicts of interest exist in the submission of this manuscript, and all authors have approved the manuscript for publication and submission to the journal.

References

1. Follak, S.; Belz, R.; Bohren, C.; De Castro, O.; Del Guacchio, E.; Pascual-Seva, N.; Schwarz, M.; Verloove, F.; Essl, F. Biological Flora of Central Europe: *Cyperus esculentus* L. *Perspect. Plant Ecol. Evol. Syst.* **2016**, *23*, 33–51. [\[CrossRef\]](#)
2. Ezech, O.; Gordon, M.H.; Niranjana, K. Yellow Nutsedge (*Cyperus esculentus*) Growth and Reproduction in Response to Nitrogen and Irrigation. *Eur. J. Lipid Sci. Technol.* **2014**, *116*, 783–794. [\[CrossRef\]](#)
3. Peerzada, A.M. Biology, Agricultural Impact, and Management of *Cyperus rotundus* L.: The World's Most Tenacious Weed. *Acta Physiol. Plant* **2017**, *39*, 270. [\[CrossRef\]](#)
4. Bohren, C.; Wirth, J. Implementation of Control Strategies against Yellow Nutsedge (*Cyperus esculentus* L.) into Practice. *J. L. KüHn-Arch.* **2018**, *458*, 189–197. [\[CrossRef\]](#)
5. Nwosu, L.C.; Edo, G.I.; Özgör, E. The Phytochemical, Proximate, Pharmacological, GC-MS Analysis of *Cyperus esculentus* (Tiger Nut): A Fully Validated Approach in Health, Food and Nutrition. *Food Biosci.* **2022**, *46*, 101551. [\[CrossRef\]](#)
6. Wang, M.; Su, Y.-Z.; Yang, R.; Yang, X. Allocation Patterns of Above- and Belowground Biomass in Desert Grassland in the Middle Reaches of Heihe River, Gansu Province, China. *Chin. J. Plant Ecol.* **2013**, *37*, 209–219. [\[CrossRef\]](#)
7. Rathore, A.C.; Kumar, A.; Tomar, J.M.S.; Jayaprakash, J.; Mehta, H.; Kaushal, R.; Alam, N.M.; Gupta, A.K.; Raizada, A.; Chaturvedi, O.P. Predictive Models for Biomass and Carbon Stock Estimation in Psidium Guajava on Bouldery Riverbed Lands in North-Western Himalayas, India. *Agrofor. Syst.* **2018**, *92*, 171–182. [\[CrossRef\]](#)
8. Das, M.; Chandra Nath, P.; Sileshi, G.W.; Pandey, R.; Nath, A.J.; Das, A.K. Biomass Models for Estimating Carbon Storage in Areca Palm Plantations. *Environ. Sustain. Ind.* **2021**, *10*, 100115. [\[CrossRef\]](#)
9. Batbaatar, A.; Carlyle, C.N.; Bork, E.W.; Chang, S.X.; Cahill, J.F. Differential Sensitivity of Above- and Belowground Plant Biomass to Drought and Defoliation in Temperate Grasslands. *Agric. Ecosyst. Environ.* **2023**, *356*, 108660. [\[CrossRef\]](#)
10. Gebremeskel, D.; Birhane, E.; Rannestad, M.M.; Gebre, S.; Tesfay, G. Biomass and Soil Carbon Stocks of Rhamnus Prinoidea Based Agroforestry Practice with Varied Density in the Drylands of Northern Ethiopia. *Agrofor. Syst.* **2021**, *95*, 1275–1293. [\[CrossRef\]](#)
11. Nie, X.; Yang, Y.; Yang, L.; Zhou, G. Above- and Belowground Biomass Allocation in Shrub Biomes across the Northeast Tibetan Plateau. *PLoS ONE* **2016**, *11*, e0154251. [\[CrossRef\]](#) [\[PubMed\]](#)

12. Peng, F.; Xue, X.; You, Q.; Sun, J.; Zhou, J.; Wang, T.; Tsunekawa, A. Change in the Trade-off between Aboveground and Belowground Biomass of Alpine Grassland: Implications for the Land Degradation Process. *Land Degrad. Dev.* **2020**, *31*, 105–117. [\[CrossRef\]](#)
13. Peng, Y.; Fornara, D.A.; Yue, K.; Peng, X.; Peng, C.; Wu, Q.; Ni, X.; Liao, S.; Yang, Y.; Wu, F.; et al. Globally Limited Individual and Combined Effects of Multiple Global Change Factors on Allometric Biomass Partitioning. *Glob. Ecol. Biogeogr.* **2022**, *31*, 454–469. [\[CrossRef\]](#)
14. Webster, T.M. Mulch Type Affects Growth and Tuber Production of Yellow Nutsedge (*Cyperus esculentus*) and Purple Nutsedge (*Cyperus rotundus*). *Weed Sci.* **2005**, *53*, 834–838. [\[CrossRef\]](#)
15. Barko, J.W.; Smart, R.M. The Growth and Biomass Distribution of Two Emergent Freshwater Plants, *Cyperus esculentus* and *Scirpus validus*, on Different Sediments. *Aquat. Bot.* **1978**, *5*, 109–117. [\[CrossRef\]](#)
16. Li, B.; Shibuya, T.; Yogo, Y.; Hara, T. Effects of Ramet Clipping and Nutrient Availability on Growth and Biomass Allocation of Yellow Nutsedge. *Ecol. Res.* **2004**, *19*, 603–612. [\[CrossRef\]](#)
17. Westendorff, N.d.R.; Agostinetto, D.; da Ulguim, A.R.; Perboni, L.T.; da Silva, B.M. Yield Loss and Economic Thresholds of Yellow Nutsedge in Irrigated Rice as a Function of the Onset of Flood Irrigation. *Bragantia* **2014**, *73*, 32–38. [\[CrossRef\]](#)
18. Larue, F.; Fumey, D.; Rouan, L.; Soulié, J.-C.; Roques, S.; Beurier, G.; Luquet, D. Modelling Tiller Growth and Mortality as a Sink-Driven Process Using Ecomeristem: Implications for Biomass Sorghum Ideotyping. *Ann. Bot.* **2019**, *124*, 675–690. [\[CrossRef\]](#)
19. Veenstra, R.L.; Messina, C.D.; Berning, D.; Haag, L.A.; Carter, P.; Hefley, T.J.; Prasad, P.V.V.; Ciampitti, I.A. Tiller Biomass in Low Plant-Density Corn Enhances Transient C Sink without Direct Harvest Index Detriment. *Field Crops Res.* **2023**, *292*, 108804. [\[CrossRef\]](#)
20. Ding, Y.; Zhang, X.; Ma, Q.; Li, F.; Tao, R.; Zhu, M.; Li, C.; Zhu, X.; Guo, W.; Ding, J. Tiller Fertility Is Critical for Improving Grain Yield, Photosynthesis, and Nitrogen Efficiency in Wheat. *J. Integr. Agric.* **2023**, *22*, 2054–2066. [\[CrossRef\]](#)
21. Xie, W.; Furusawa, C.; Miyata, H.; Ata-Ul-Karim, S.T.; Yamasaki, Y.; Shiotsu, F.; Kato, Y. Genotypic Differences in the Agronomic Performance of Ratoon Rice in a Cool-Temperate Environment in Central Japan. *Field Crops Res.* **2024**, *317*, 109487. [\[CrossRef\]](#)
22. Dimobe, K.; Goetze, D.; Ouédraogo, A.; Mensah, S.; Akpagana, K.; Porembski, S.; Thiombiano, A. Aboveground Biomass Allometric Equations and Carbon Content of the Shea Butter Tree (*Vitellaria Paradoxa* C.F. Gaertn., Sapotaceae) Components in Sudanian Savannas (West Africa). *Agrofor. Syst.* **2019**, *93*, 1119–1132. [\[CrossRef\]](#)
23. Bem, C.M.; Cargnelutti Filho, A.; Faccio, G.; Schabaram, D.E.; Silveira, D.L.; Simões, F.M.; Uliana, D.B. Growth Models for Morphological Traits of Sunn Hemp. *Semin. Agrar.* **2016**, *38*, 2933. [\[CrossRef\]](#)
24. Eker, M.; Poudel, K.; Özçelik, R. Aboveground Biomass Equations for Small Trees of Brutian Pine in Turkey to Facilitate Harvesting and Management. *Forests* **2017**, *8*, 477. [\[CrossRef\]](#)
25. Jian, L.I.; Wang, M.; Wang, Y.; Zhang, M.; Yao, N. Fitting Model of Jilin Quinoa Growth Model Based on Meteorological Factors. *J. Jilin Agric. Univ.* **2017**, *39*, 743–747. [\[CrossRef\]](#)
26. Nyamjav, J.; Batsaikhan, M.-E.; Li, G.; Li, J.; Luvsanjamba, A.; Jin, K.; Xiao, W.; Wu, L.; Indree, T.; Qin, A. Allometric Equations for Estimating Above-Ground Biomass of *Nitraria sibirica* Pall. in Gobi Desert of Mongolia. *PLoS ONE* **2020**, *15*, e0239268. [\[CrossRef\]](#)
27. Hossain, M.; Siddique, M.R.H.; Saha, S.; Abdullah, S.M.R. Allometric Models for Biomass, Nutrients and Carbon Stock in *Excoecaria agallocha* of the Sundarbans, Bangladesh. *Wetl. Ecol. Manag.* **2015**, *23*, 765–774. [\[CrossRef\]](#)
28. Sepaskhah, A.R.; Fahandezh-Saadi, S.; Zand-Parsa, S. Logistic Model Application for Prediction of Maize Yield under Water and Nitrogen Management. *Agric. Water Manag.* **2011**, *99*, 51–57. [\[CrossRef\]](#)
29. Cheng, Y.; Wei, Z.M.; Liu, J.Y.; Xu, F.; Wang, Z.; Chen, T. Logistic Equation Based Fitting and Analysis of the Growth Index of *Cyperus esculentus*. *J. Northeast Agric. Sci.* **2024**, *49*, 47–51. [\[CrossRef\]](#)
30. Fourcaud, T.; Zhang, X.; Stokes, A.; Lambers, H.; Korner, C. Plant Growth Modelling and Applications: The Increasing Importance of Plant Architecture in Growth Models. *Ann. Bot.* **2008**, *101*, 1053–1063. [\[CrossRef\]](#)
31. Tanwar, S.P.S.; Verma, A.; Kumar, P.; Alam, N.M.; Bhatt, R.K. Biomass and Carbon Projection Models in *Hardwickia Binata* Roxb. *Vis a Vis Estimation of Its Carbon Sequestration Potential under Arid Environment. Arch. Agron. Soil Sci.* **2020**, *66*, 1925–1935. [\[CrossRef\]](#)
32. Liu, A.N.; Zhang, Y.; Hou, Z.F.; Lu, G.H. Allometric Scaling of Biomass with Nitrogen and Phosphorus Above- and below-Ground in Herbaceous Plants Varies along Water-Salinity Gradients. *AoB Plants* **2021**, *13*, plab030. [\[CrossRef\]](#) [\[PubMed\]](#)
33. Ma, X.; Wang, X. Aboveground and Belowground Biomass and Its' Allometry for *Salsola Passerina* Shrub in Degraded Steppe Desert in Northwestern China. *Land Degrad. Dev.* **2021**, *32*, 714–722. [\[CrossRef\]](#)
34. Li, Y.; Jiang, L.; liu, M.; Li, J. Simulation of Rice Biomass Accumulation by an Extended Logistic Model Including Influence of Meteorological Factors. *Int. J. Biometeorol.* **2002**, *46*, 185–191. [\[CrossRef\]](#)
35. Meade, K.A.; Cooper, M.; Beavis, W.D. Modeling Biomass Accumulation in Maize Kernels. *Field Crops Res.* **2013**, *151*, 92–100. [\[CrossRef\]](#)
36. Dou, Y.; Yang, Y.; An, S. Above-Ground Biomass Models of *Caragana Korshinskii* and *Sophora Viciifolia* in the Loess Plateau, China. *Sustainability* **2019**, *11*, 1674. [\[CrossRef\]](#)

37. Gambín, B.L.; Borrás, L.; Otegui, M.E. Kernel Weight Dependence upon Plant Growth at Different Grain-Filling Stages in Maize and Sorghum. *Aust. J. Agric. Res.* **2008**, *59*, 280. [\[CrossRef\]](#)
38. Pepler, S.; Gooding, M.J.; Ellis, R.H. Modelling Simultaneously Water Content and Dry Matter Dynamics of Wheat Grains. *Field Crops Res.* **2006**, *95*, 49–63. [\[CrossRef\]](#)
39. Song, Y.; Wan, G.-Y.; Wang, J.-X.; Zhang, Z.-S.; Xia, J.-Q.; Sun, L.-Q.; Lu, J.; Ma, C.-X.; Yu, L.-H.; Xiang, C.-B.; et al. Balanced Nitrogen–Iron Sufficiency Boosts Grain Yield and Nitrogen Use Efficiency by Promoting Tillering. *Mol. Plant* **2023**, *16*, 2004–2010. [\[CrossRef\]](#)
40. Okamura, M.; Aoki, N. Effect of Two Alleles of Tiller Angle Control 1 on Grain Yield and Dry Matter Production in Rice. *Field Crops Res.* **2024**, *309*, 109325. [\[CrossRef\]](#)
41. Li, J.; Han, G.; Kang, S.; Zhang, X.; Li, C. Responses of Tillering Stipa Breviflora Traits to a Long-Term Grazing Gradient. *Acta Soc. Bot. Pol.* **2022**, *91*, 13. [\[CrossRef\]](#)
42. Křen, J.; Klem, K.; Svobodová, I.; Miša, P.; Neudert, L. Yield and Grain Quality of Spring Barley as Affected by Biomass Formation at Early Growth Stages. *Plant Soil Environ.* **2014**, *60*, 221–227. [\[CrossRef\]](#)
43. Boe, A.; Beck, D.L. Yield Components of Biomass in Switchgrass. *Crop Science* **2008**, *48*, 1306–1311. [\[CrossRef\]](#)
44. R: The R Project for Statistical Computing. Available online: <https://www.r-project.org/> (accessed on 28 December 2024).
45. Kuhn, M. Building Predictive Models in R Using the Caret Package. *J. Stat. Softw.* **2008**, *28*, 1–26. [\[CrossRef\]](#)
46. Isler, K.; Barbour, A.D.; Martin, R.D. Line-Fitting by Rotation: A Nonparametric Method for Bivariate Allometric Analysis. *Biom. J.* **2002**, *44*, 289. [\[CrossRef\]](#)
47. Pareja, G. *Fitting a Logistic Curve to Population Size Data*; Iowa State University: Ames, IA, USA, 1984. [\[CrossRef\]](#)
48. Winsor, C.P. The Gompertz Curve as a Growth Curve. *Proc. Natl. Acad. Sci. USA* **1932**, *18*, 1–8. [\[CrossRef\]](#) [\[PubMed\]](#)
49. Bayen, P.; Noulèkoun, F.; Bognounou, F.; Lykke, A.M.; Faso, B. Models for Estimating Aboveground Biomass of Four Dryland Woody Species in Burkina Faso, West Africa. *J. Arid. Environ.* **2020**, *180*, 104205. [\[CrossRef\]](#)
50. Shu, M.; Shen, M.; Dong, Q.; Yang, X.; Li, B.; Ma, Y. Estimating the Maize Above-Ground Biomass by Constructing the Tridimensional Concept Model Based on UAV-Based Digital and Multi-Spectral Images. *Field Crop. Res.* **2022**, *282*, 108491. [\[CrossRef\]](#)
51. Mello, A.; Toebe, M.; Marchioro, V.S.; de Souza, R.R.; Paraginski, J.A.; Somavilla, J.C.; Martins, V.; Manfio, G.L.; Junges, D.L.; da Rocha Borges, M.E. Nonlinear Models in the Description of Sunflower Cultivars Growth Considering Heteroscedasticity. *J. Plant Growth Regul.* **2023**, *42*, 7215–7228. [\[CrossRef\]](#)
52. Niklas, K.J. Modelling Below- and Above-Ground Biomass for Non-Woody and Woody Plants. *Ann. Bot.* **2005**, *95*, 315–321. [\[CrossRef\]](#)
53. Chaturvedi, R.K.; Raghubanshi, A.S. Allometric Models for Accurate Estimation of Aboveground Biomass of Teak in Tropical Dry Forests of India. *For. Sci.* **2015**, *61*, 938–949. [\[CrossRef\]](#)
54. Weiner, J. Allocation, Plasticity and Allometry in Plants. *Perspect. Plant Ecol. Evol. Syst.* **2004**, *6*, 207–215. [\[CrossRef\]](#)
55. Prusinkiewicz, P. Modeling Plant Growth and Development. *Curr. Opin. Plant Biol.* **2004**, *7*, 79–83. [\[CrossRef\]](#)
56. Nguimkeu, P. A Simple Selection Test between the Gompertz and Logistic Growth Models. *Technol. Forecast. Soc. Change* **2014**, *88*, 98–105. [\[CrossRef\]](#)
57. Wang, W.; Quanjiu, W.; Jun, F.; Lijun, S.; Xinlei, S. Logistic Model Analysis of Winter Wheat Growth on China’s Loess Plateau. *Can. J. Plant Sci.* **2014**, *94*, 1471–1479. [\[CrossRef\]](#)
58. de Bem, C.M.; Cargnelutti Filho, A.; Chaves, G.G.; Kleinpaul, J.A.; Pezzini, R.V.; Lavezo, A. Gompertz and Logistic Models to the Productive Traits of Sunn Hemp. *JAS* **2017**, *10*, 225. [\[CrossRef\]](#)
59. Ma, J.; Yuan, C.; Zhou, J.; Li, Y.; Gao, G.; Fu, B. Logistic Model Outperforms Allometric Regression to Estimate Biomass of Xerophytic Shrubs. *Ecol. Indic.* **2021**, *132*, 108278. [\[CrossRef\]](#)
60. Randriamalala, J.R.; Radosy, H.O.; Ramanakoto, M.; Razafindrahanta, H.; Ravoninjatovo, J.-M.; Haingomanantsoa, R.S.; Ramanantoandro, T. Allometric Models to Predict the Individual Aboveground Biomass of Shrubs of Malagasy Xerophytic Thickets. *J. Arid. Environ.* **2022**, *202*, 104751. [\[CrossRef\]](#)
61. Kuyah, S.; Sileshi, G.W.; Rosenstock, T.S. Allometric Models Based on Bayesian Frameworks Give Better Estimates of Aboveground Biomass in the Miombo Woodlands. *Forests* **2016**, *7*, 13. [\[CrossRef\]](#)
62. Saha, C.; Mahmood, H.; Nayan, S.N.S.; Siddique, M.R.H.; Abdullah, S.M.R.; Islam, S.M.Z.; Iqbal, M.Z.; Akhter, M. Allometric Biomass Models for the Most Abundant Fruit Tree Species of Bangladesh: A Non-Destructive Approach. *Environ. Chall.* **2021**, *3*, 100047. [\[CrossRef\]](#)
63. Liu, R.; Yang, X.; Gao, R.; Hou, X.; Huo, L.; Huang, Z.; Cornelissen, J.H.C. Allometry Rather than Abiotic Drivers Explains Biomass Allocation among Leaves, Stems and Roots of Artemisia across a Large Environmental Gradient in China. *J. Ecol.* **2021**, *109*, 1026–1040. [\[CrossRef\]](#)
64. Carini, F.; Filho, A.C.; Bandeira, C.T.; Neu, I.M.M.; Pezzini, R.V.; Pacheco, M.; Thomasi, R.M. Growth Models for Lettuce Cultivars Growing in Spring. *J. Agric. Sci.* **2017**, *11*, 147. [\[CrossRef\]](#)

65. Connor, D.J.; Fereres, E. A Dynamic Model of Crop Growth and Partitioning of Biomass. *Field Crops Res.* **1999**, *63*, 139–157. [[CrossRef](#)]
66. Zhang, H.; Zhao, Y.; Zhu, J.-K. Thriving under Stress: How Plants Balance Growth and the Stress Response. *Dev. Cell* **2020**, *55*, 529–543. [[CrossRef](#)]
67. Lin, Z.; Fan, D.; Ma, S.; Miao, W.; Wang, X. Relative Growth Rate for Trees at the Growth Stage Is Coordinated with Leaf Bulk Modulus of Elasticity and Osmotic Potential in a Subtropical Forest of China. *Ecol. Indic.* **2022**, *141*, 109135. [[CrossRef](#)]
68. Li, G.; Si, M.; Zhang, C.; Shen, Z.; Wang, S.; Shao, J. Responses of Plant Biomass and Biomass Allocation to Experimental Drought: A Global Phylogenetic Meta-Analysis. *Agric. For. Meteorol.* **2024**, *347*, 109917. [[CrossRef](#)]
69. Acciari, H.A.; Guamet, J.J. Below- and Above-ground Growth and Biomass Allocation in Maize and Sorghum Halepense in Response to Soil Water Competition. *Weed Res.* **2010**, *50*, 481–492. [[CrossRef](#)]
70. Dolezal, J.; Jandova, V.; Macek, M.; Liancourt, P. Contrasting Biomass Allocation Responses across Ontogeny and Stress Gradients Reveal Plant Adaptations to Drought and Cold. *Funct. Ecol.* **2021**, *35*, 32–42. [[CrossRef](#)]
71. Deprá, M.S.; Lopes, S.J.; Noal, G.; Reiniger, L.R.S.; Cocco, D.T. Modelo Logístico de Crescimento de Cultivares Crioulas de Milho e de Progenies de Meios-Irmãos Maternos Em Função Da Soma Térmica. *Cienc. Rural.* **2016**, *46*, 36–43. [[CrossRef](#)]
72. Noulèkoun, F.; Khamzina, A.; Naab, J.B.; Lamers, J.P.A. Biomass Allocation in Five Semi-Arid Afforestation Species Is Driven Mainly by Ontogeny Rather than Resource Availability. *Ann. Sci.* **2017**, *74*, 78. [[CrossRef](#)]
73. Soliveres, S.; Maestre, F.T. Plant–Plant Interactions, Environmental Gradients and Plant Diversity: A Global Synthesis of Community-Level Studies. *Perspect. Plant Ecol. Evol. Syst.* **2014**, *16*, 154–163. [[CrossRef](#)]
74. Cleland, E.E.; Lind, E.M.; DeCrappeo, N.M.; DeLorenze, E.; Wilkins, R.A.; Adler, P.B.; Bakker, J.D.; Brown, C.S.; Davies, K.F.; Esch, E.; et al. Belowground Biomass Response to Nutrient Enrichment Depends on Light Limitation Across Globally Distributed Grasslands. *Ecosystems* **2019**, *22*, 1466–1477. [[CrossRef](#)]
75. Ma, X.; Wang, X. Biomass Partitioning and Allometric Relations of the Reaumuria Soongorica Shrub in Alxa Steppe Desert in NW China. *For. Ecol. Manag.* **2020**, *468*, 118178. [[CrossRef](#)]
76. Xu, H.; Wang, Z.; Li, Y.; He, J.; Wu, X. Dynamic Growth Models for Caragana Korshinskii Shrub Biomass in China. *J. Environ. Manag.* **2020**, *269*, 110675. [[CrossRef](#)] [[PubMed](#)]
77. Naik, S.K.; Sarkar, P.K.; Das, B.; Singh, A.K.; Bhatt, B.P. Biomass Production and Carbon Stocks Estimate in Mango Orchards of Hot and Sub-Humid Climate in Eastern Region, India. *Carbon. Manag.* **2019**, *10*, 477–487. [[CrossRef](#)]
78. Ge, H.; Yuepeng, S.; Xuehui, S.; Deqiang, Z.; Xiaoyu, Z. Optimal Growth Model of Populus Simonii Seedling Combination Based on Logistic and Gompertz Models. *bjlydxxb* **2020**, *42*, 59–70. [[CrossRef](#)]
79. Li, Y.; Jiang, L.; Liu, M. A Nonlinear Mixed-Effects Model to Predict Stem Cumulative Biomass of Standing Trees. *Procedia Environ. Sci.* **2011**, *10*, 215–221. [[CrossRef](#)]

Disclaimer/Publisher’s Note: The statements, opinions and data contained in all publications are solely those of the individual author(s) and contributor(s) and not of MDPI and/or the editor(s). MDPI and/or the editor(s) disclaim responsibility for any injury to people or property resulting from any ideas, methods, instructions or products referred to in the content.